Large Igneous Provinces: A Driver of Environmental and Biotic Changes (AGU Geophysical Monograph 255)

Was the Kalkarindji continental flood basalt province a driver of environmental change at the dawn of the Phanerozoic?

Short Title: Kalkarindji: Environmental change in the Cambrian?

Authors: Peter E. Marshall*[a], Luke E. Faggetter[b], Mike Widdowson[c]

[a]Fugro GeoServices Ltd, Armstrong House, Unit 43, Number 1 Industrial Estate, Consett, DH8 6TW, UK.

[b]School of Earth and Environment, University of Leeds, Leeds, LS2 9JT, UK.

[c]Department of Geography, Environment and Earth Sciences, University of Hull, Hull, HU6 7RX, UK.

*Corresponding author:

Dr Peter Marshall, email: petermarshall202@gmail.com

Abstract

The Kalkarindji continental flood basalt province of Northern Australia is the oldest basaltic LIP in the Phanerozoic having erupted in the mid Cambrian. At this time, during the Cambrian Explosion, the global environment suffered a series of mass extinctions and biotic turnover. Kalkarindji had the potential to release 1.65 x 10^6 Tg of CO_2, approximately 1.72% of the total Cambrian atmospheric carbon reservoir. It has therefore been implicated as a driver of the environmental changes in the Cambrian Series 2. However, temporal discrepancies between Kalkarindji eruptions and biotic turnover may prevent this LIP from being attributed as the sole cause of the Botomian-Toyonian Extinction, which wiped out up to 45% of all genera in the fossil record; whilst environmental factors such as sea-level change causing ocean anoxia are implicated in the Redlichiid-Olenellid Extinction. It is certainly possible that Kalkarindji could have played a part in forcing these environmental changes, but further advances in geochronology and sedimentary volcanic proxies are needed to confidently define a direct causational link between these events at the dawn of the Phanerozoic.

Keywords

Kalkarindji; flood lava volcanism; environmental change; Cambrian; Series 2

1. Introduction

Identifying triggers of environmental change in the early Cambrian is a key component in understanding how our planet transitioned during the early Palaeozoic.. The apparently consistent coincidence of large igneous provinces and mass extinction events throughout geological history (Courtillot and Renne, 2003; Bond and Wignall, 2014) does make it appealing to label this correlation as a causational link (Keller, 2005). However, as at other intervals in time (K-Pg boundary; Renne et al., 2015), this may not be a straightforward causal relationship.

Even though traditionally the Cambrian, at the dawn of the Phanerozoic, has taken centre stage as the crucible of modern animals, the advent of macroscopic life is rooted in the earlier Ediacaran period (Droser and Gehling, 2015; Smith et al., 2016; Zhu et al., 2017). At the onset of the Phanerozoic, global diversity radiated in two distinct intervals: the first 20 million years of the Cambrian (known as the Cambrian Explosion), and again during the Great Ordovician Biodiversification Event (GOBE; Sepkoski, 1979, 1996; Zhu et al., 2006; Bambach et al., 2007; Servais et al., 2008). Broadly, the transition from the Cambrian Explosion to the GOBE represents a shift from initial "explosive" evolution to "boom and bust" during the GOBE. Earth had transitioned from extreme icehouse in the Cryogenian to the extreme greenhouse conditions of the Cambrian; this transition also equates to a peak in modelled atmospheric CO_2 levels for the Phanerozoic (Berner, 2006) and felsic volcanism (Mckenzie et al., 2014, 2016). Effectively, this means the role of a single LIP in forcing environmental change**.** and it's relation to extinction events must be viewed through the lens of long-term tectonic and biotic activity.

While it is unlikely a single LIP can account for the broad biotic and abiotic trends in the geological record of the early Phanerozoic alone, the temporal coincidence of continental volcanism with evidence for extinction and environmental stress in the Cambrian**.** Series 2 renders it an essential interval to assess the links between these phenomena. At this time, the fossil record documents the step-wise proliferation of enigmatic new body plans and the exploration of ecological niches and the resultant co-evolution of life and environment (Maloof et al., 2010). Despite this apparent 'explosion' of metazoan life, there is clear evidence for inherent instability in the Cambrian environment, with two pertinent examples in the Cambrian Series 2 succession (Zhuravlev and Wood, 1996, 2018; Montañez et al., 2000; Babcock et al., 2015). The first major biotic crisis in the Cambrian, the Botomian-Toyonian Extinction (BTE.), triggered a decline in global generic diversity (~45% genera loss; Sepkoski, 1996). Following the BTE, dominant trilobite faunas from Laurentia and Gondwana were replaced at the Series 2 – Miaolingian (previously known as the Cambrian Series 3; see the Subcommission on Cambrian Stratigraphy) boundary (Montañez et al., 2000; Zhu et al., 2006). These events have been speculatively linked to the emplacement of the Kalkarindji continental flood basalt province (CFBP) (Glass and Phillips, 2006; Jourdan et al., 2014), which erupted onto the Gondwanan continent in the mid-Cambrian, making this the oldest LIP in the Phanerozoic (Marshall et al., 2018; Ware and Jourdan, 2018). Kalkarindji magmatism appears in apparent synchrony with disruption to the Cambrian carbon cycle, recorded as a large negative carbon isotope excursion (the Redlichiid-Olenellid Extinction Carbon isotope Excursion.; ROECE.) at the Series 2 – Miaolingian boundary (Montañez et al., 2000; Zhu et al., 2006; Faggetter et al., 2016, 2017; Chang et al., 2017; Ren et al., 2018). As the link between Kalkarindji and these biotic phenomena is still in debate, this chapter discusses the evidence, potential and possibility of Kalkarindji as a driver of extinction and environmental change in the mid Cambrian.

2. The Kalkarindji Continental Flood Basalt Province

Kalkarindji currently exists as a scattered collection of five individual sub-provinces: the Antrim Plateau (APV), Helen Springs (HSV), Nutwood Downs (NDV), Peaker Piker and Colless (PPC), and Table Hill Volcanics (THV) as well as various intrusive dykes spread across Northern Territory, Western Australia, South Australia and NW Queensland (Fig. 1). By far the largest sub-province, the Antrim Plateau Volcanics (c. 50,000 km^2 with a maximum lava pile thickness of 1.10 km) is composed mainly of undifferentiated aphyric basaltic andesite with four minor, recognisable members contained within the basalt pile: the Blackfella Rockhole Member, Bingy Bingy Basalt Member, Mt Close Chert and Malley Springs Sandstone members (Mory and Beere, 1985; Marshall et al., 2016). The intercalated sediment members occur in localised areas of the province and indicate periods of volcanic repose and marine/lacustrine inundation of the lava pile. The APV unconformably overlies Proterozoic sandstone basin units and Archean basement fragments of the North Australian Craton (NAC; Sweet et al., 1974a, 1974b; Scott et al., 2000). The vast majority of lava flows range from 5 - 50 m thickness, are near flat-lying and have been subject to little to no tectonic influence. The APV is overlain by sedimentary units of shallow basins formed through the late Cambrian to Cretaceous (Kruse and Munson, 2013a, 2013b, 2013c).

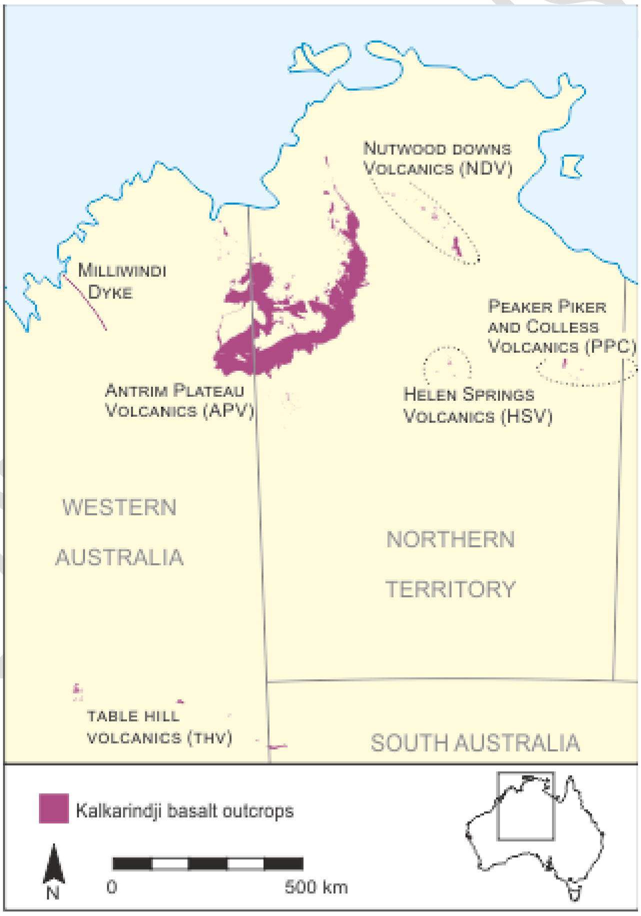

__Figure 1:__ Map of modern day exposure of Kalkarindji. basalt outcrop.

The entire Kalkarindji covers, in total, an estimated 55,000 km^2 (Bultitude, 1972, 1976; Marshall, 2015) and if the northern sub provinces were originally connected as a single contiguous lava field, they would have had an original estimated areal extent of ~ 400,000 km^2 (Veevers, 2001), with an estimated volume. of ~1.5×10^5 km^3 (Marshall et al., 2016). Previous size estimates of > 2×10^6 km^3 (Glass and Phillips, 2006; Evins et al., 2009; Jourdan et al., 2014) assume a blanket lava flow coverage of not only the current extrusive remnants, but also those wider peripheral areas currently underlain by sills and/or dykes with similar geochemical affinity, resulting in a postulated extrusive cover extending over half of Australia. Size estimates from Marshall (2015) follow the more realistic postulate that such a widespread blanket lava flow coverage is unlikely. The THV lie over 1000 km south of the APV, and as yet, no extrusive lava flows, vent sites or other physical indication suggests these two provinces are fragments of a once uninterrupted lava field. Lava flows are seldom seen to flow the distances between the APV and THV due to the cooling effects of the atmosphere; a rare example being the Rajahmundry Traps of Eastern India (Self et al., 2008). Here, similar areal extent arguments were originally made for outliers of the Deccan province, but were later shown to be fed by either separate eruptive centres, or in very rare the case of the Rajahmundry Traps, narrow topographically-channelised flows. Dyke systems however, are commonly known to propagate over long distances (Ernst et al., 2001; Hou, 2012), extending beyond the extrusive limit of basaltic LIPs due to their insulation in the country rock.

Detailed field mapping of the volcanic successions from basement to overlying sediment at locations in the east and west of the APV (Marshall, 2015), indicates that little of the original extrusive material has been lost due to erosion in the APV. Arguably the amount of material lost from other sub-provinces would also be minimal. This together with the fact that extensive drilling of the Officer Basin has only located intrusive dolerites, but no extrusive basalt, mitigates against these geographically separate regions being once covered by a single uninterrupted lava field.

Given that each sub-province corresponds to a different pre-existing basin with differing volcanic architecture and barriers of basement topography highs directly overlain by younger Cambrian sediments between each basin (Marshall, 2015), it is seems probable that some volcanic sub-provinces of Kalkarindji-type magmatism developed geographically independent, and that each was fed from a broader, sub-lithospheric source through their own individual system of dykes and volcanic centres. To summarise, they are related to one another by a remarkably homogenous geochemistry and age, which indicates a single regional magmatic event, but the intrusive and extrusive components currently identified do not together represent erosionally-separated remnants of a once single widespread CFBP.

2.1. Geochemistry

The Kalkarindji basalts are low-Ti tholeiitic basalts (Bultitude, 1976; Glass and Phillips, 2006), characterised by relatively low FeO, a low CaO/Al_2O_3 ratio and relatively high SiO_2 values compared to typical Mid Ocean Ridge Basalts (MORB). The first geochemical studies of the province were made during the first initial mapping of the volcanics of Northern Territory (Bultitude, 1972, 1976), collecting samples from the APV, HSV and NDV. These samples indicated that all the volcanics were basalt and basaltic andesites, and although a likely correlation between these extrusive provinces was inferred, no direct geographical link was made.

Glass and Phillips (2006) first highlighted the unique homogeneity of Kalkarindji, that unlike other oft-studied CFBPs, these flows all have a relatively homogenous signature irrespective of stratigraphical position or geographical location (Fig. 2). The lavas display a consistent fractionation signature, suggesting a common parentage of a single magma source evolving throughout the lifetime of eruption, rather than derivation from multiple sub-lithospheric sources. Thus the near identical trace element chemistry allowed Glass (2002), to confidently define these scattered provinces as a single magmatic event with a common parentage and provided the 'Kalkarindji CFBP' appellation to describe the whole province.

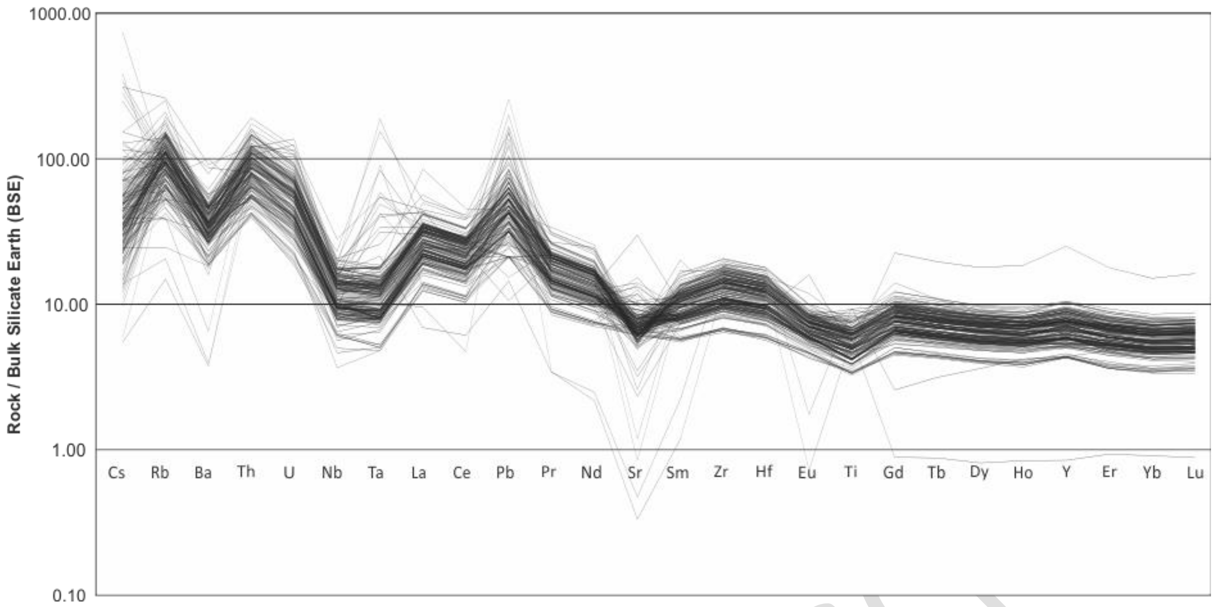

Figure 2: *Multi-element diagram normalised to bulk silicate Earth, showing Kalkarindji samples plot on a highly repeatable, uniquely homogenous signature for most elements. Cs, Ba, Ta, Pb and Sr show significant variation between samples indicative of alteration. Data collected from Glass, 2002; Evins et al., 2009; Marshall, 2015.*

The lavas are enriched in LILE, LREE and Pb indicating significant crustal contamination of the magma has occurred before eruption of lavas began, during which time fractional crystallisation of the magma reservoir has occurred. Marshall (2015) matched fractionation trends with those produced through modelling the crystallisation from a primitive parental magma, to infer fractionation occurred between 0.1 - 0.3 GPa which equates to roughly 5 - 10 km depth. The later stage lavas do not exhibit evolved signatures, indicating magma recharge into the reservoir throughout its lifetime. Interestingly the lavas show clear fractionation of Cr and Ni, yet no olivine or Cr-spinel are identified in mineralogy. Have these earlier crystal phases been retained at magma source? A depletion in Cu suggests sulphur sequestration of chalcophile elements from the magma may also have occurred through interaction with a sulphur rich crustal component (Keays and Lightfoot, 2010), although no suitable basement unit has yet been found that might satisfy this conundrum.

The Kalkarindji basalts can be distinguished from typical tholeiites by their depleted high-field strength element (HFSE) signatures (Ti, P, Nb) relative to incompatible elements and an extreme enrichment in the highly incompatible elements (Th, U, LREE) (Glass, 2002; Marshall, 2015; Ware, 2017). Despite

Kalkarindji being more evolved, this depletion is a feature shared with other flood basalt provinces (Peate and Hawkesworth, 1996), and may indicate a common magma generation origin among CFBPs. By contrast, the trace element signature is most likely indicative of crustal contamination to a similar degree as other provinces, thus the evolved signature is a product of a source material inferred to be more evolved than primitive mantle. Ware et al. (2018) posit this evolved signature derives from an ancient subcontinental lithospheric mantle (SCLM) becoming enriched by either metasomatised fluid percolation or subducted sediment contamination around 2.5 Ga.

Alteration is pervasive throughout the exposed outcrop across the whole Kalkarindji province. Physical weathering is typically moderate to extreme, with local conditions such as proximity to fault lines and modern topography most likely to have the greatest influence on the level of alteration. Yet, chemical alteration on a whole-rock scale is apparently minimal (the constituent elements seeming to have been largely immobile with the exception of LILE and Sr); by contrast on a crystallographic scale, minerals and elements have obviously been lost and replaced (Marshall, 2015). An explanation for this is that the hydrothermal alteration to have affected the Kalkarindji can be viewed as a near closed system. Fluids entering the system leached, and mobilised specific elements with secondary growth of clays initiated by the need to precipitate elements into a solid state, largely as sericite, saussurite, chlorite and opaque Fe-oxides.

The overall outcome of this process is that the bulk chemistry does not significantly deviate from a typical tholeiitic basaltic andesite signature. The chemical alteration is low and nearly undetectable in many indices of alteration, only marginally affecting the Kalkarindji basalt chemistry.

The typical volatiles of CO_2 and SO_2 produced from Kalkarindji are relatively low for a CFBP, analogous to Columbia River outputs. Using the area and volume estimations above and the volume calculations of Marshall et al. (2016), the total SO_2 produced from the whole Kalkarindji eruptive phase would be 9.07×10^5 Tg whilst the total CO_2 produced is 1.65×10^6 Tg (at 80% degassing efficacy), approximately 1.72% of the total Cambrian atmospheric CO_2 reservoir, which has been modelled at 32x pre-industrial levels (PAL; Hearing et al., 2018). With a continuous average eruption rate of 1000 m^3s^{-1}, the total mass of basalt would have been erupted in 4,757 years. However, continuity of eruption is unlikely given periods of volcanic repose indicated by intercalated sediment members identified in the APV. and HSV. The effectiveness of delivery to the global atmospheric reservoir is also restricted by the lack of evidence for an extensive explosive APV eruptive stage, thus reducing the likelihood of efficient volcanic plumes that might have been able to penetrate the tropopause and initiate global effects (Marshall et al., 2016); although explosive eruptions cannot be wholly dismissed due to the potential erosion of material from the lava pile.

2.2. Age of Magmatism

Bultitude (1972) first inferred a temporal relationship between the Kalkarindji. sub-provinces by reporting similar K-Ar dates from the NDV and HSV. Glass (nee Hanley) further confirmed the existence of a single magmatic event through the correlation of absolute radiometric dating of the Milliwindi Dyke of northern Western Australia (WA), HSV and APV (Hanley and Wingate, 2000; Glass and Phillips, 2006). This homogeneity was corroborated further by Evins et al. (2009) who demonstrated the Table Hill Volcanics of southern WA to be near identical in their geochemistry and age. Further dating of associated intrusives (Macdonald et al., 2005; Jourdan et al., 2014; Ware and Jourdan, 2018) and extrusives (Marshall et al., 2018) point toward a complex, extended magmatic history, beginning with intrusion into the Australian cratonic basement around 512 Ma, with final eruption of the APV occurring between 509 - 498 Ma (Marshall et al., 2018). Magmatism is likely to have been driven by decompressional partial melting of an already warmed source material (due to edge-driven convection around the stable cratonic roots of the North Australian Craton) caused in part by the torsional stresses applied by the rapid rotation of the Gondwanan continent in the early Phanerozoic (Ware et al., 2018).

3. Palaeo-environment

The NAC stabilised around 1750 Ma, forming a key part of the Proterozoic supercontinent Rodinia**.**. Along with other cratons to the west (Pilbara and Yilgarn) and south (Gawler and Nullarbor) this formed the stable cratonic environment which underlies much of the Australian continent (Scott et al., 2000). In the Mesoproterozoic a series of complex intracratonic polyphase basins (Officer, Amadeus, Ngalia and Georgina), collectively termed the Centralian Superbasin (CS) - a useful, but somewhat oversimplified generalisation - covered the majority of these ancient terranes across Australia's western interior (Walter et al., 1995; Walter and Veevers, 1997; Lindsay et al., 2005). The formation of the CS around 800 Ma is most likely attributable to crustal sag in response to the uplift and subsequent decline from superplume activity beneath the Australian cratons generating large volumes of clastic material (Lindsay, 2002). Compressional dynamics prevailed in the Neoproterozoic and the CS was restructured into a series of largely independent foreland basins separated by uplifted basement blocks (Munson et al., 2013; Schmid, 2017). The CS is infilled with a succession of Neoproterozoic - Palaeozoic sediments, mostly sandstones and carbonates that provide an excellent record of metazoan radiation in the early Cambrian (Lindsay et al., 2005; Creveling et al., 2014).

At the Cambrian Series 2 – Miaolingian boundary (~509 Ma) Australia was positioned at a low, equatorial latitude on the north-eastern periphery of Gondwana (Fig. 3; Torsvik and Cocks, 2009). At this time, the various Kalkarindji**.** sub-provinces covered extensive parts of the CS with variably thick subaerial basalts. Evidence of disparate intercalated sediment deposition within the basalt successions indicates that Kalkarindji was erupted at/near to the coastline. This emplacement triggered widespread lithospheric subsidence, initiating broad swathes of equatorial, shallow epeiric seaways which spread inland, eventually creating the Ord, Wiso, Daly and Georgina basins (Munson et al., 2013; Schmid, 2017). Post Kalkarindji eruption, these basins were characterised by the deposition of shallow marine carbonate and mixed carbonate-siliciclastic successions (Kruse and Munson, 2013a, 2013b, 2013c). These successions have well-described and diverse regional faunas that can, with some degree of success, be correlated across these different basins thus inferring the establishment of an open shallow sea-way on the north-eastern periphery of Gondwana.

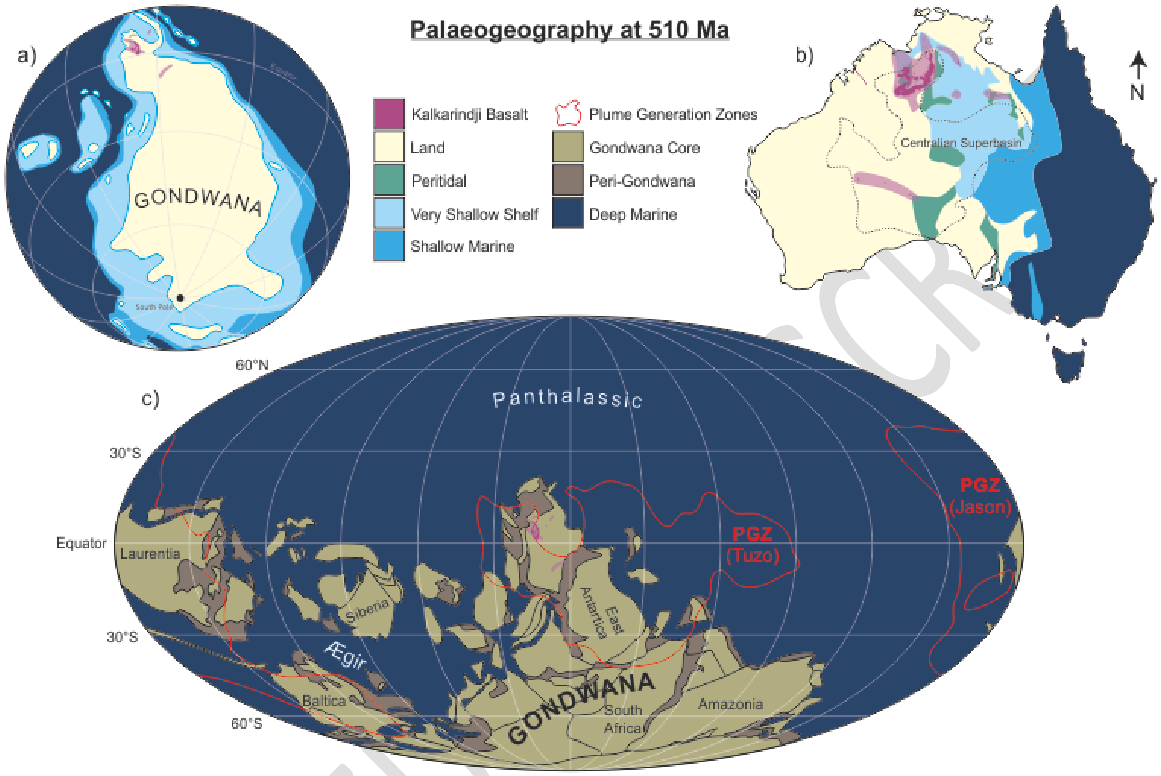

__Figure 3:__ __a)__ Orthographic projection of Gondwana. showing approximate position of Kalkarindji. LIP (modified from Torsvik and Cocks, 2009). __b)__ Approximate position of Kalkarindji LIP and other associated volcanic units, the position of the Centralian Superbasin (dashed line) and the distribution of marine facies at 510 Ma illustrating transgression (modified from Munson et al., 2013). __c)__ Palaeogeographic reconstruction showing approximate position of the Kalkarindji LIP and the Plume Generation Zones (PGZ) active at 510 Ma (modified from Torsvik and Cocks, 2017).

4. Linked bioenvironmental phenomena in the Cambrian Series 2

4.1. Biotic instability

Global diversity in the early Palaeozoic began with an initial radiation during the first 20 million years of the Cambrian., commonly known as the "Cambrian Explosion" (Sepkoski, 1979; Zhu et al., 2006; Bambach et al., 2007; Servais et al., 2008) occurring within two distinct phases, separated by significant environmental and biotic events (Zhuravlev and Wood, 2018). Despite the evident proliferation of life, two critical intervals of major genera-level losses and taxonomic turnover appear in apparent synchrony with the Kalkarindji (Zhuravlev and Wood, 1996; Faggetter et al., 2017). The first occurred in the late Series 2 when, at the acme of widespread construction of archaeocyathan reef morphologies, this recently established diversity and habitability crashed. The remarkable diversification witnessed in the Fortunian and Stage 2 was abruptly halted by the Sinsk Event (~516 Ma) - a decline in global generic diversity in archaeocyathan reefs and in the off-reef Tommotian fauna, marking the onset of the BTE (Brasier, 1996; Zhuravlev and Wood, 1996). The Sinsk Event is linked to the widespread encroachment of deep water anoxia onto the shallow-marine shelves (Zhuravlev and Wood, 1996, 2018; Ivantsov et al., 2005; He et al., 2019). Later, the Hawke Bay Regression Event (HBRE), marks the final BTE extinction interval. The HBRE killed off the remaining archaeocyath populations, severely affecting hyoliths, and endemic, shallow marine trilobites (Brasier, 1996; Zhuravlev and Wood, 1996).

The second significant biotic turnover. in the Cambrian. Series 2 involved the olenellid trilobites of Laurentia and redlichiid trilobites of Gondwana. Despite trilobites undergoing widespread radiation from the Cambrian Series 2 onward, there was significant replacement of dominant faunas known as biomeres. Specifically the Olenellid biomere at the Cambrian Series 2 – Miaolingian boundary on Laurentia which marks the sudden disappearance of olenellids in the fossil record (Palmer, 1998; Webster et al., 2008). Though no rigorous attempts to fit multiple sections recording the olenellid extinction within a sequence stratigraphic framework as-yet exists, preliminary evidence suggests that the last appearance of the Olenellids displays a close temporal association with the Sauk I/Sauk II boundary, but occurs during a deepening succession deposited onto the Laurentian continent (Faggetter, 2017). On Gondwana the redlichiid trilobites also did not survive long-after the onset of the Miaolingian (Zhu et al., 2004, 2006; Smith et al., 2015), the interval of their disappearance coincided with a major transgression (sea-level rise) onto the continent (Southgate and Shergold, 1991). A negative carbon isotope excursion (ROECE) marks the disappearance of these trilobite species and has been used as a geochemical marker for the Series 2 – Miaolingian boundary strata (Zhu et al., 2006). This boundary is seen to be worldwide with sections logged in Scotland (Faggetter et al., 2016), China (Guo et al., 2010; Chang et al., 2017; Ren et al., 2017), Australia (Schmid, 2017) and the USA where it coincides with the upper boundary of the Olenellid biomere (Montañez et al., 2000; Faggetter et al., 2017). Previous suggestions by Brasier (1996) depict olenellid-redlichiid extinction and the BTE as a single event, however, this may have persisted as a timing discrepancy later clarified by compiled $\delta^{13}C$ chemostratigraphies and the distinction between ROECE and the BTE associated MICE/AECE isotopic excursions (Zhu et al., 2006).

Kalkarindji volcanism, ocean anoxia and sea level change have all been implicated in driving both the BTE**.** and the olenellid-redlichiid extinction event (Zhuravlev and Wood, 1996; Palmer, 1998; Montañez et al., 2000; Jourdan et al., 2014). However, the close temporal association between volcanism and environmental change indicators (either biotic or environmental) alone do not provide empirical evidence that regions experiencing extinction and environmental stress were so affected by volcanic activity. Dates for the Kalkarindji range from c. 510 - 500 Ma (Fig. 4; Marshall et al., 2018), and so indicate that the Kalkarindji is too young to have been an instigating factor in driving the BTE, which culminated in the Toyonian at ~512 Ma (Brasier, 1996; Zhuravlev and Wood, 1996; Ogg et al., 2016). This presents two problems when correlating these events. Firstly, the lack of a ratified radiometric age for the Cambrian Series 2– Miaolingian boundary means comparative studies are based on undefined ages and, secondly, inherent error from radioisotopic methods makes precise correlation between the Kalkarindji LIP and extinction challenging. It is also important to note that mass extinctions are generally defined as geologically brief intervals (~1 Ma) during which extinction rates are elevated considerably beyond background rates, and during which diverse taxa from a broad range of habitats are affected worldwide (Hallam and Wignall, 1997). Certainly, the BTE fits this description (~45% generic loss), yet the olenellid-redlichiid extinction at the Series 2 – Miaolangian boundary can be ascribed to a lesser extinction event following faunal turnover and a shift to dominantly agnostoid trilobite faunas (Babcock et al., 2017) implying a biomere boundary rather than a true mass extinction.

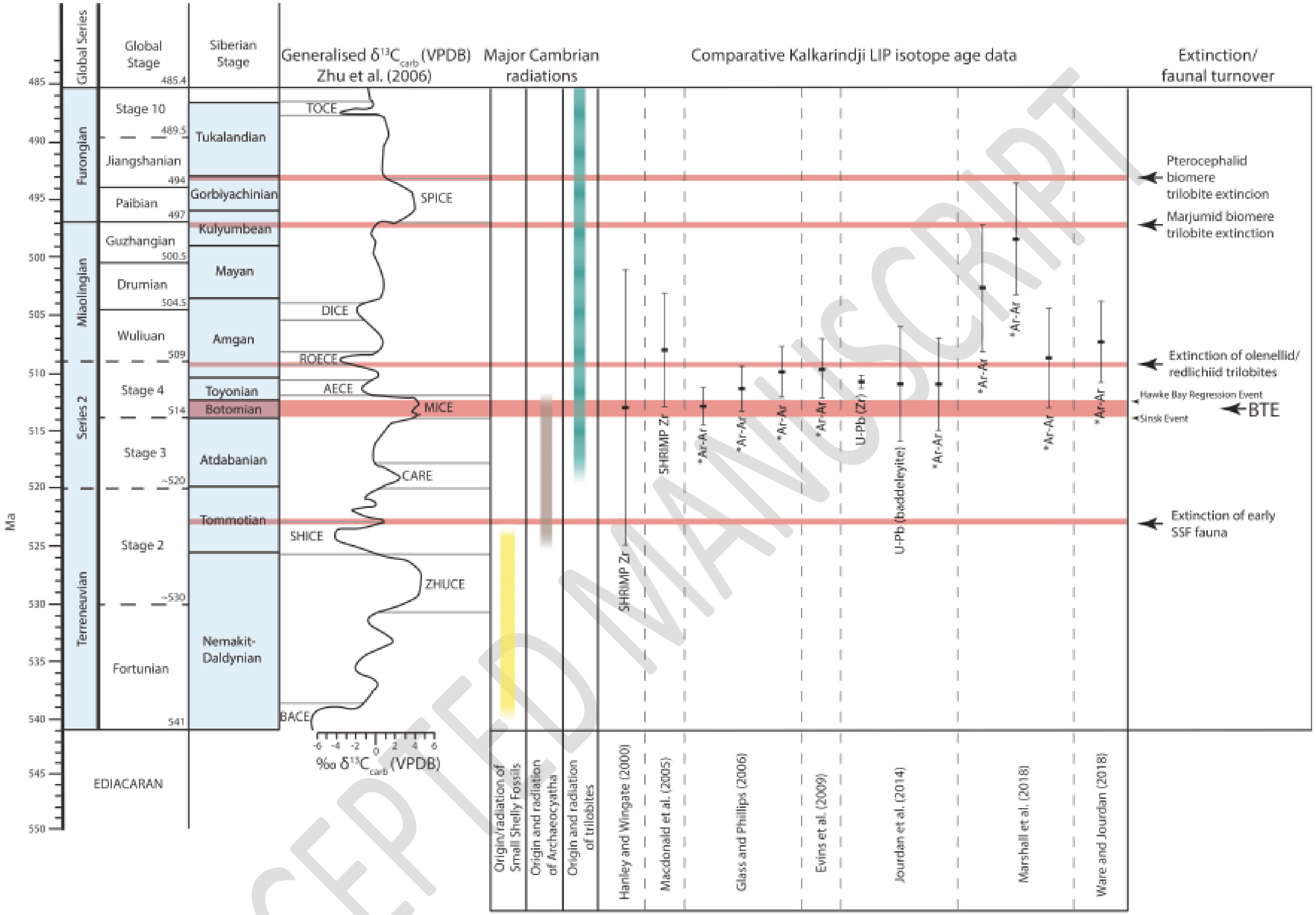

Figure 4: *Cambrian chronostratigraphy, major evolutionary radiations, extinctions and Kalkarindji. LIP dates. Dates marked with an asterisk indicate isotope ages recalibrated to Renne et al. (2010). Cambrian timescale from Cohen et al. (2018); generalised inorganic carbon isotope curve and Cambrian extinctions from Zhu et al. (2006); SSF range from Maloof et al. (2010); origin and radiation of archaocyatha from Zhuravlev (1996) and Zhuravlev and Wood, (1996); origin and radiation of trilobites from Kouchinsky et al. (2012). Approximate Extinction age of Small Shelly Fossils (SSFs) from Maloof et al. (2010); BTE from Zhuravlev and Wood (1996); olenellid/redlichiid. from Zhu et al. (2006); Marjumid biomere and Pterocephalid biomere from Gerhardt and Gill (2016).*

4.2. Environmental instability

Global environmental instability is inherent in the Cambrian as a combined consequence of multiple phenomena often rooted in the Proterozoic including; continental landmasses amalgamating into the Gondwanan supercontinent (Svensen et al., 2017), continental denudation and transgression (Peters and Gaines, 2012), dynamic weathering regimes (Squire et al., 2006), increasing continental arc volcanism (Mckenzie et al., 2014), changing ocean circulation (Tucker, 1992) and evolving seawater chemistry (Brennan et al., 2004). Following the global diversity decline observed from the upper Series 2until the Series 2 – Miaolingian boundary, it has been suggested that the globally synchronous trend of decreasing $\delta^{13}C$ values of seawater, characterised as ROECE, reflects the culmination of a long-term biomass decline and subsequent reduction of the burial flux of organic matter (Guo et al., 2010; Zhang et al., 2015; Chang et al., 2017; Ren et al., 2017; Schmid, 2017). However, It is also possible that ROECE is not only driven by coincident biomass decline, but that there is also an underlying control exerted by longer-term tectonic regimes relating to carbonate weathering (Shields and Mills, 2017). Regardless of the ultimate driving factor, the positioning of ROECE within transgression implies that the shallowing of oxygen depleted bottom waters may have contributed toward a negative shift in $\delta^{13}C$ values (Creveling et al., 2014; Feng et al., 2014; Zhang et al., 2015; Jin et al., 2016; Schmid, 2017). Creveling et al. (2014) and Schmid (2017) depict second-order transgressive cycles deposited onto the Australian continent under a spectrum of anoxic conditions, including euxinic and ferruginous intervals. Whilst Zhang et al. (2015) note a sharp increase in the abundance and spatial distribution of microbial oncoidal carbonates at the Series 2 – Miaolingian boundary in China. Although no *in situ* $\delta^{13}C$ values are reported, a temporal association of this microbial resurgence with the Series 2 – Miaolingian boundary interval (and extrapolation to ROECE) suggest a link to ocean anoxia.

Further tertiary evidence for severe environmental disruption coincident with the Kalkarindji LIP and the BTE/redlichiid-olenellid extinction is elucidated by $\delta^{34}S$ values and sulphate concentrations in francolite-bound sulphate from Series 2 – Miaolingian boundary carbonates in Australia. Here Hough et al. (2006) find a sharp $\delta^{34}S$ rise across the Series 2 – Miaolingian boundary interval, ascribing this to a significant increase in pyrite burial fluxes, suggested to result from increased pyrite formation within the water column and the spread of anoxia caused by the shallowing of deep, anoxic waters over continental shelves and carbonate platforms during transgression events. However, it is important to note that these high values are not entirely characteristic of this interval world-wide, and other studies (Wotte et al., 2007, 2012) suggest that $\delta^{34}S$ values described in Hough et al. (2006) may be a reflection of the restricted nature of Australian epeiric seaways in the Cambrian. Still, shoaling of oxygen depleted water remains consistent with the interpretation that ROECE records or coincides with the shallowing of oxygen-depleted bottom waters onto shallow marine shelves following a protracted period of biomass decline in the upper Series 2. Extended intervals of marine anoxia are often associated with warmer ocean temperatures due to the diminished capacity for warmer water to store dissolved oxygen (Hough et al., 2006). Records of warm sea surface temperatures (Wotte et al., 2019), a global greenhouse climate (Hearing et al., 2018; Zhuravlev and Wood, 2018) and potential global warming indicated by deposition of extensive carbonate and evaporite deposits (Keller et al., 2012; Schmid, 2017) are evident during the window of time for the Kalkarindji emplacement. During this period of the spread of ocean anoxia may have rendered shallow marine environments potentially vulnerable to CH_4 and/or H_2S poisoning during transgression. Hough et al. (2006) posit the influx of vast CO_2 into the atmosphere from Kalkarindji as a plausible kill mechanism tied to global diversity loss in the upper Series 2 and at the Series 2 – Miaolingian boundary. Whilst these authors' evidence and hypothesis seem to fit other examples of LIP-extinction coincidence during the Phanerozoic, the potential for their data to distinguish between the BTE and trilobite extinction remains elusive, as is evidence that this scenario occurred within strata recording extinction.

Fluctuating $^{87}Sr/^{86}Sr$ seawater values have long alluded to major secular ocean chemical variations in the Cambrian, during which the highest $^{87}Sr/^{86}Sr$ values of the previous 900 myr are recorded close to the Series 2– Miaolingian boundary (Montañez et al., 1996, 2000; Peters and Gaines, 2012; Wotte et al., 2012). A complex $^{87}Sr/^{86}Sr$ history characterises the early Cambrian and depicts a long-term (~350 myr) rise culminating in the Cambrian Terreneuvian, punctuated by an abrupt fall at the Cambrian Series 2 – Miaolingian boundary, and returning to rising values in the late Miaolingian and Furongian (Montañez et al., 1996, 2000). This abrupt, short-term (~4 myr) downturn close to the Series 2 – Miaolingian boundary was ascribed by Montañez et al. (2000) as the plausible result of increased weathering fluxes of young, mantle-derived mafic rocks and speculatively attributed to an increase in hydrothermal Sr fluxes due to continental rifting in the latest Series 2. Crucially, Montañez et al. (2000) reveal the timing of decreasing $^{87}Sr/^{86}Sr$ seawater values as strongly corresponding to the current age framework for the Kalkarindji and the position of ROECE at the Series 2 – Miaolingian boundary. The significant loss of Sr from the Kalkarindji basalts (Marshall, 2015) also ties in with this theory, raising the possibility that the source driving the abrupt downturn of $^{87}Sr/^{86}Sr$ seawater values at the Series 2 – Miaolingian is the weathering of newly emplaced basalts of the Kalkarindji LIP. Although Montañez (2000) provide a relatively low-resolution framework, this displays a strong temporal coincidence to the BTE and redlichiid-olenellid extinction.

5. Summary

The Kalkarindji likely erupted as a relatively modest-sized CFBP, probably comparable in extent to the Columbia River Basalts of NW USA. The eruption appears to have been broadly synchronous with two biotic crises in the Cambrian Series 2. In entirety the lavas had the potential to release gases amounting to 1 - 2% of the global Cambrian atmospheric carbon reservoir, an amount with potential to enact environmental change. However, the rate of release during the volcanic episode, together with the efficacy of delivery to the atmosphere are likely to have mitigated against delivering any rapid or profound environmental change. The proposed environmental repercussions include the BTE and olenellid-redlichiid extinctions, the ROECE (although longer-term biomass decline and regional redox regime change is more likely responsible) and an abrupt lowering of the oceanic Sr ratios. Although these events are clearly supported by their respective data-sets, a coincidence of timing does not uniquely establish LIP volcanism as the driving mechanism, largely because no irrefutable *in situ* evidence links a volcanic signature to these phenomena within the same stratigraphy.

Undoubtedly discussion regarding the LIP-mass extinction link in the Cambrian has been aided through continually improving precision of stratigraphical correlations, the ability to distinguish between different extinction events, and the advancement of radiometric dating of volcanic successions. There is now an increasing amount of evidence, that the emplacement of Kalkarindji was closely coincident with environmental change in the Cambrian, but whether this represents the sole, or primary cause of mass extinctions remains unproven.

Accordingly, further geochronological studies are essential, as is establishing a sedimentary proxy for volcanism in strata recording extinction phenomena. Investigations into the relatively unknown impact of intrusive magmatism on environmental volatile budgets, either through volatile release through shallow intrusions or thermal effects upon country rock, are required. Such information may prove significant in a province where the majority of magmatism is suspected to have been intrusive.

Establishment of a clear link to volcanism would provide the “smoking gun” that LIP volcanism is inexorably linked with mass extinction events in the early Phanerozoic. Here, the application of Hg as a tracer for volcanism is becoming increasingly successful in showing links between volcanism, ocean anoxia, climate change and extinction (as discussed in Section III of this Monograph). However, recent studies investigating deep time application of Hg as a proxy for volcanism highlights the complexity of the proxy (Faggetter et al., 2019), discuss the processes affecting Hg cycling (e.g. redox; Pruss et al., 2019) and behaviour during diagenesis (Percival et al., 2018), and should therefore be applied with scrutiny and consideration of wholistic biogeochemical cycles.

Acknowledgements

This work is a result of a collaboration between the PhD research of both Peter Marshall at the Open University and Luke Faggetter at the University of Leeds. Fieldwork was conducted in 2012 and 2013 by P. Marshall, L. Faggetter and M. Widdowson. Funding for this research was provided by the Open University, Proto Resources and Investments, and the Natural Environment Research Council (NERC). Many thanks to S. Kelley, D. Murphy, S. Sherlock, C. Mac Niocaill, P. Wignall and R. Newton for assistance and discussion. We particularly acknowledge N. Hughes, F. Jourdan and two anonymous reviewers for their insightful reviews and comments that aided in improving this manuscript.

References

Babcock, L.E., Peng, S., Ahlberg, P. (2017). Cambrian trilobite biostratigraaphy and its role in developing an integrated history of the Earth System. *Lethaia* **50**, 381–399.

Babcock, L.E., Peng, S.C., Brett, C.E., Zhu, M.Y., Ahlberg, P., Bevis, M., Robinson, R.A. (2015). Global climate, sea level cycles, and biotic events in the Cambrian Period. *Palaeoworld* **24**, 5–15.

Bambach, R.K., Bush, A.M., Erwin, D.H. (2007). Autecology and the filling of ecospace: key metazoan radiations. *Palaeontology* **50**, 1–22.

Berner, R.A. (2006). GEOCARBSULF: a combined model for Phanerozoic atmospheric O_2 and CO_2. *Geochim. Cosmochim. Acta* **70**, 5653–5664.

Bond, D.P.G., Wignall, P.B. (2014). Large igneous provinces and mass extinctions: An update. *Geol. Soc. Am. Spec. Pap.* **505**, 29–55. https://doi.org/10.1130/2014.2505(02).

Brasier, M.D. (1996). The basal Cambrian transition and Cambrian bio-events (from terminal Proterozoic extinctions to Cambrian biomeres), in: *Global Events and Event Stratigraphy in the Phanerozoic*. Springer, Berlin, Heidelberg, pp. 113–138.

Brennan, S.T., Lowenstein, T.K., Horita, J. (2004). Seawater chemistry and the advent of biocalcification. *Geology* **32**, 473–476.

Bultitude, R.J. (1972). The Geology and Petrology of the Helen Springs, Nutwood Downs, and Peaker Piker Volcanics. *Bur. Miner. Resour. Geol. Geophys.* **1972/74**.

Bultitude, R.J. (1976). Flood basalts of probable early Cambrian age in northern Australia, in: Johnson, R.W. (Ed.), *Volcanism in Australasia*. Canberra, pp. 1–20.

Chang, C., Hu, W., Wang, X., Yu, H., Yang, A., Cao, J., Yao, S. (2017). Carbon isotope stratigraphy of the lower to middle Cambrian on the eastern Yangtze Platform, South China. *Palaeogeogr. Palaeoclimatol. Palaeoecol.* **479**, 90–101. https://doi.org/10.1016/j.palaeo.2017.04.019.

Cohen, K.M., Finney, S.C., Gibbard, P.L., Fan, J.-X. (2018). The ICS International Chronostratigraphic Chart. *Episodes* **36**, 199–204.

Courtillot, V.E., Renne, P.R. (2003). On the ages of flood basalt events. *Comptes Rendus Geosci.* **335**, 113–140. https://doi.org/10.1016/S1631-0713(03)00006-3.

Creveling, J.R., Johnston, D.T., Poulton, S.W., Kotrc, B., Marz, C., Schrag, D.P., Knoll, A. (2014). Phosphorus sources for phosphatic Cambrian carbonates. *Geol. Soc. Am. Bull.* **126**, 145–163.

Droser, M.L., Gehling, J.G. (2015). The advent of animals, the view from the Ediacaran. *Proc. Natl. Acad. Sci.* **112**, 4865–4870.

Ernst, R.E., Grosfils, E.B., Mège, D. (2001). Giant Dyke Swarms: Earth, Venus, and Mars. *Annu. Rev. Earth Planet. Sci.* **29**, 489–534.

Evins, L.Z., Jourdan, F., Phillips, D. (2009). The Cambrian Kalkarindji Large Igneous Province: Extent and characteristics based on new ^{40}Ar/^{39}Ar and geochemical data. *Lithos* **110**, 294–304. https://doi.org/10.1016/j.lithos.2009.01.014.

Faggetter, L.E. (2017). *Environmental change, trilobite extinction and massive volcanism at the Cambrian Series 2 – Series 3 boundary*. PhD Thesis. University of Leeds.

Faggetter, L.E., Wignall, P.B., Pruss, S.B., Jones, D.S., Grasby, S., Widdowson, M., Newton, R.J., Science, E., Lane, W., Ls, L., Kingdom, U. (2019). Mercury chemostratigraphy across the Cambrian Series 2 – Series 3 boundary: evidence for increased volcanic activity coincident with extinction? *Chem. Geol.* **510**, 188–199. https://doi.org/10.1016/j.chemgeo.2019.02.006.

Faggetter, L.E., Wignall, P.B., Pruss, S.B., Newton, R.J., Sun, Y., Crowley, S.F. (2017). Trilobite extinctions, facies changes and the ROECE carbon isotope excursion at the Cambrian Series 2-3 boundary, Great Basin, western USA. *Palaeogeogr. Palaeoclimatol. Palaeoecol.* **478**, 53–66. https://doi.org/10.1016/j.palaeo.2017.04.009.

Faggetter, L.E., Wignall, P.B., Pruss, S.B., Sun, Y., Raine, R.J., Newton, R.J., Widdowson, M., Joachimski, M.M., Smith, P.M. (2016). Sequence stratigraphy, chemostratigraphy and facies analysis of Cambrian Series 2 – Series 3 boundary strata in northwestern Scotland. *Geol. Mag.* 1–13. https://doi.org/10.1017/S0016756816000947.

Feng, L., Li, C., Huang, J., Chang, H., Chu, X. (2014). A sulfate control on marine mid-depth euxinia on the early Cambrian (ca. 529–521 Ma) Yangtze platform, South China. *Precambrian Res.* **246**, 123–133.

Gerhardt, A.M., Gill, B.C. (2016). Elucidating the relationship between the later Cambrian end-Marjuman extinctions and SPICE Event. *Palaeogeogr. Palaeoclimatol. Palaeoecol.* **461**, 362–373.

Glass, L.M. (2002). *Petrogenesis and Geochronology of the North Australian Kalkarinji Low-Ti Continental Flood Basalt Province*. PhD Thesis. Australian National University.

Glass, L.M., Phillips, D. (2006). The Kalkarindji continental flood basalt province: A new Cambrian large igneous province in Australia with possible links to faunal extinctions. *Geology* **34**, 461–464. https://doi.org/10.1130/G22122.1.

Guo, Q., Strauss, H., Liu, C., Zhao, Y., Yang, X., Peng, J., Yang, H. (2010). A negative carbon isotope excursion defines the boundary from Cambrian Series 2 to Cambrian Series 3 on the Yangtze Platform, South China. *Palaeogeogr. Palaeoclimatol. Palaeoecol.* **285**, 69–88.

Hallam, A., Wignall, P.B. (1997). *Mass Extinctions and Their Aftermath*. Oxford University Press.

Hanley, L.M., Wingate, M.T.D. (2000). SHRIMP zircon age for an Early Cambrian dolerite dyke: An intrusive phase of the Antrim Plateau Volcanics of northern Australia. *Aust. J. Earth Sci.* **47**, 1029–1040. https://doi.org/10.1046/j.1440-0952.2000.00829.x.

He, T., Zhu, M., Mills, B., Wynn, P., Zhuravlev, A., Tostevin, R., Pogge von Strandmann, P., Yang, A., Poulton, S., Shields, G. (2019). Possible links between extreme oxygen perturbations and the Cambrian radiation of animals. *Nat. Geosci.*

Hearing, T.W., Harvey, T.H.P., Williams, M., Leng, M.J., Lamb, A.L., Wilby, P.R., Gabbott, S.E., Pohl, A., Donnadieu, Y. (2018). An early Cambrian greenhouse climate. *Sci. Adv.* **4**, eaar5690.

Hou, G. (2012). Mechanism for three types of mafic dyke swarms. *Geosci. Front.* **3**, 217–223. https://doi.org/10.1016/j.gsf.2011.10.003.

Hough, M.L., Shields, G.A., Evins, L.Z., Strauss, H., Henderson, R.A., Mackenzie, S. (2006). A major sulphur isotope event at c. 510 Ma: a possible anoxia-extinction-volcanism connection during the Early-Middle Cambrian transition? *Terra Nov.* **18**, 257–263. https://doi.org/10.1111/j.1365-3121.2006.00687.x.

Ivantsov, A.Y., Zhuravlev, A.Y., Leguta, A. V., Krassilov, V.A., Melnikova, L.M., Ushatinskaya, G.T. (2005). Palaeoecology of the early Cambrian Sinsk biota from the Siberian platform. *Palaeogeogr. Palaeoclimatol. Palaeoecol.* **220**, 69–88.

Jin, C., Li, C., Algeo, T.J., Planavsky, N.J., Cui, H., Yang, X., Xie, S. (2016). A highly redox-heterogeneous ocean in South China during the early Cambrian (~529–514 Ma): Implications for biota environmentco-evolution. *Earth Planet. Sci. Lett.* **441**, 38–51.

Jourdan, F., Hodges, K., Sell, B., Schaltegger, U., Wingate, M.T.D., Evins, L.Z., Soderlund, U., Haines, P.W., Phillips, D., Blenkinsop, T. (2014). High-precision dating of the Kalkarindji large igneous province, Australia, and synchrony with the Early-Middle Cambrian (Stage 4-5) extinction. *Geology* **42**, 543–546. https://doi.org/10.1130/G35434.1.

Keays, R.R., Lightfoot, P.C. (2010). Crustal sulfur is required to form magmatic Ni-Cu sulfide deposits: Evidence from chalcophile element signatures of Siberian and Deccan Trap basalts. *Miner. Depos.* **45**, 241–257. https://doi.org/10.1007/s00126-009-0271-1.

Keller, G. (2005). Impacts, volcanism and mass extinction: random coincidence or cause and effect? *Aust. J. Earth Sci.* **52**, 725–757. https://doi.org/10.1080/08120090500170393.

Keller, M., Cooper, J.D., Lehnert, O. (2012). *Sauk megasequence supersequences, southern Great Basin: second-order accommodation events on the southwestern Cordilleran margin platform*.

Kouchinsky, A., Bengtson, S., Runnegar, B., Skovsted, C., Steiner, M., Vendrasco, M. (2012). Chronology of early Cambrian biomineralization. *Geol. Mag.* **149**, 221–251.

Kruse, P., Munson, T. (2013a). Ord Basin, in: Ahmad, M., Munson, T.J. (Eds.), *Geology and Mineral Resources of the Northern Territory*. Northern Territory Geological Survey, Darwin, pp. 33:1-33:10.

Kruse, P., Munson, T. (2013b). Daly Basin, in: Ahmad, M., Munson, T. (Eds.), *Geology and Mineral Resources of the Northern Territory*. Northern Territory Geological Survey, Darwin, pp. 31:1-31:13.

Kruse, P., Munson, T. (2013c). Wiso Basin, in: Ahmad, M., Munson, T.J. (Eds.), *Geology and Mineral Resources of the Northern Territory*. Northern Territory Geological Survey, Darwin, pp. 32:1-32:11.

Lindsay, J.F. (2002). Supersequences, superbasins, supercontinents - evidence from the Neoproterozoic-Early Palaeozoic basins of central Australia. *Basin Res.* **14**, 207–223. https://doi.org/10.1046/j.1365-2117.2002.00170.x.

Lindsay, J.F., Kruse, P.D., Green, O.R., Hawkins, E., Brasier, M.D., Cartlidge, J., Corfield, R.M. (2005). The Neoproterozoic – Cambrian record in Australia : A stable isotope study. *Precambrian Res.* **143**, 113–133. https://doi.org/10.1016/j.precamres.2005.10.002.

Macdonald, F.A., Wingate, M.T.D., Mitchell, K. (2005). Geology and age of the Glikson impact structure, Western Australia. *Aust. J. Earth Sci.* **52**, 641–651. https://doi.org/10.1080/08120090500170419.

Maloof, A.C., Porter, S.M., Moore, J.L., Dudás, F.Ö., Bowring, S.A., Higgins, J.A., Fike, D.A., Eddy, M.P. (2010). The earliest Cambrian record of animals and ocean geochemical change. *Bull. Geol. Soc. Am.* **122**, 1731–1774. https://doi.org/10.1130/B30346.1.

Marshall, P.E. (2015). *The Volcanic Architecture, Geochemistry and Geochronology of the Kalkarindji Continental Flood Basalt Province, Australia*. PhD Thesis. The Open University.

Marshall, P.E., Halton, A.M., Kelley, S.P., Widdowson, M., Sherlock, S.C. (2018). New $^{40}Ar/^{39}Ar$ dating of the Antrim Plateau Volcanics, Australia: clarifying an age for the eruptive phase of the Kalkarindji continental flood basalt province. *J. Geol. Soc. London.* **175**, 974–985. https://doi.org/10.1144/jgs2018-035.

Marshall, P.E., Widdowson, M., Murphy, D.T. (2016). The Giant Lavas of Kalkarindji: rubbly pāhoehoe lava in an ancient continental flood basalt province. *Palaeogeogr. Palaeoclimatol. Palaeoecol.* **441**, 22–37. https://doi.org/10.1016/j.palaeo.2015.05.006.

Mckenzie, N.R., Horton, B.K., Loomis, S.E., Stockli, D.F., Planavsky, N.J., Lee, C.-T.A. (2016). Continental arc volcanism as the principal driver of icehouse-greenhouse variability. *Science (80-.).* **352**, 444–447. https://doi.org/10.1126/science.aad5787.

Mckenzie, N.R., Hughes, N.C., Gill, B.C., Myrow, P.M. (2014). Plate tectonic influences on Neoproterozoic-early Paleozoic climate and animal evolution. *Geology* **42**, 127–130. https://doi.org/10.1130/G34962.1.

Montañez, I.P., Banner, J.L., Osleger, D.A., Borg, L.E., Bosserman, P.J. (1996). Integrated Sr isotope variations and sea-level history of Middle to Upper Cambrian platform carbonates: Implications for the evolution of Cambrian seawater $^{87}Sr/^{86}Sr$. *Geology* **24**, 917–920.

Montañez, I.P., Osleger, D.A., Banner, J.L., Mack, L.E., Musgrove, M. (2000). Evolution of the Sr and C isotope composition of Cambrian oceans. *GSA Today* **10**, 1–6.

Mory, A.J., Beere, G.M. (1985). Palaeozoic stratigraphy of the Ord Basin, Western Australia and Northern Territory. *Geol. Surv. West. Aust. Artic.* **14**, 36–45.

Munson, T.J., Kruse, P.D.D., Ahmad, M. (2013). Centralian Superbasin, in: Ahmad, M., Munson, T.J. (Eds.), *Geology and Mineral Resources of the Northern Territory*. Northern Territory Geological Survey, Northern Territory Geological Survey, Darwin, pp. 22:1-22:20.

Ogg, J.G., Ogg, G., Gradstein, F.M. (2016). *A Concise Geologic Time Scale*. Elsevier, Amsterdam. https://doi.org/10.1016/B978-0-444-59467-9.00005-4.

Palmer, A.R. (1998). Terminal early Cambrian extinction of the Olenellina: documentation from the Pioche Formation, Nevada. *J. Paleontol.* **72**, 650–672.

Peate, D.W., Hawkesworth, C.J. (1996). Lithospheric to asthenospheric transition in low-Ti flood basalts from southern Paraná, Brazil. *Chem. Geol.* **127**, 1–24. https://doi.org/10.1016/0009-2541(95)00086-0.

Percival, L.M., Jenkyns, H.C., Mather, T.A., Dickson, A.J., Batenburg, S.J., Ruhl, M., Hesselbo, S., Barclay, R., Jarvis, I., Robinson, S.., Woelders, L. (2018). Does large igneous province volcanism always perturb the mercury cycle? Comparing the records of Oceanic Anoxic Event 2 and the end-Cretaceous to other Mesozoic events. *Am. J. Sci.* **318**, 799–860. https://doi.org/10.2475/08.2018.01.

Peters, S.E., Gaines, R.R. (2012). Formation of the 'Great Unconformity as a trigger for the Cambrian explosion. *Nature* **484**, 363.

Pruss, S.B., Jones, D.S., Fike, D.A., Tosca, N.J., Wignall, P.B. (2019). Marine anoxia and sedimentary mercury enrichments during the Late Cambrian SPICE event in northern Scotland. *Geology*.

Ren, Y., Zhong, D., Gao, C., Li, B., Cao, X., Wang, A., Dong, Y., Yan, T. (2018). The paleoenvironmental evolution of the Cambrian Longwangmiao Formation (Stage 4, Toyonian) on the Yangtze Platform, South China: Petrographic and geochemical constrains. *Mar. Pet. Geol.* https://doi.org/10.1016/j.marpetgeo.2018.10.022.

Ren, Y., Zhong, D., Gao, C., Liang, T., Sun, H., Wu, D., Zheng, X. (2017). High-resolution carbon isotope records and correlations of the lower Cambrian Longwangmiao formation (stage 4, Toyonian) in Chongqing, South China. *Palaeogeogr. Palaeoclimatol. Palaeoecol.*

Renne, P.R., Mundil, R., Balco, G., Min, K., Ludwig, K.R., Mundil, R., Min, K. (2010). Joint determination of 40K decay constants and 40Ar∗/40K for the Fish Canyon sanidine standard, and improved accuracy for 40Ar/39Ar geochronology. *Geochim. Cosmochim. Acta* **74**, 5349–5367. https://doi.org/10.1016/j.gca.2010.06.017.

Renne, P.R., Sprain, C.J., Richards, M.A., Self, S., Vanderkluysen, L., Pande, K. (2015). State shift in Deccan volcanism at the Cretaceous-Paleogene boundary, possibly induced by impact. *Science (80-.).* **350**, 76–78. https://doi.org/10.1126/science.aac7549.

Schmid, S. (2017). Chemostratigraphy and palaeo-environmental characterisation of the Cambrian stratigraphy in the Amadeus Basin, Australia. *Chem. Geol.* **451**, 169–182.

Scott, D.L., Rawlings, D.J., Page, R.W., Tarlowski, C.Z., Idnurm, M., Jackson, M.J., Southgate, P.N. (2000). Basement framework and geodynamic evolution of the Palaeoproterozoic superbasins of north-central Australia: An integrated review of geochemical, geochronological and geophysical data. *Aust. J. Earth Sci.* **47**, 341–380. https://doi.org/10.1046/j.1440-0952.2000.00793.x.

Self, S., Jay, A.E., Widdowson, M., Keszthelyi, L.P. (2008). Correlation of the Deccan and Rajahmundry Trap lavas: Are these the longest and largest lava flows on Earth? *J. Volcanol. Geotherm. Res.* **172**, 3–19. https://doi.org/10.1016/j.jvolgeores.2006.11.012.

Sepkoski, J.J. (1979). A kinetic model of Phanerozoic taxonomic diversity II. Early Phanerozoic families and multiple equilibria. *Paleobiology* **5**, 222–251.

Sepkoski, J.J. (1996). *Patterns of Phanerozoic extinction: a perspective from global data bases. In Global events and event stratigraphy in the Phanerozoic*. Springer.

Servais, T., Lehnert, O., Li, J.U.N., Mullins, G.L., Munnecke, A., Nuetzel, A., Vecoli, M. (2008). The Ordovician Biodiversification: revolution in the oceanic trophic chain. *Lethaia* **41**, 99–109.

Shields, G.A., Mills, B.J. (2017). Tectonic controls on the long-term carbon isotope mass balance. *Proc. Natl. Acad. Sci.* **114**, 4318–4323.

Smith, E.F., Nelson, L.L., Strange, M.A., Eyster, A.E., Rowland, S.M., Schrag, D.P., Macdonald, F.A. (2016). The end of the Ediacaran: Two new exceptionally preserved body fossil assemblages from Mount Dunfee, Nevada, USA. *Geology* **44**, 911–914.

Smith, P.M., Brock, G.A., Paterson, J.R. (2015). Fauna and biostratigraphy of the Cambrian (Series 2, Stage 4; Ordian) Tempe Formation (Pertaoorrta Group), Amadeus Basin, Northern Territory. *Alcheringa An Australas. J. Palaeontol.* **39**, 40–70.

Southgate, P.N., Shergold, J.H. (1991). Application of sequence stratigraphic concepts to Middle Cambrian phosphogenesis, Georgina Basin, Australia. *J. Aust. Geol. Geophys.* **12**, 119–144.

Squire, R.J., Campbell, I.H., Allen, C.M., Wilson, C.J. (2006). Did the Transgondwanan Supermountain trigger the explosive radiation of animals on Earth? *Earth Planet. Sci. Lett.* **250**, 116–133.

Svensen, H.H., Torsvik, T.H., Callegaro, S., Augland, L., Heimdal, T.H., Jerram, D.A., Planke, S., Pereira, E. (2017). Gondwana Large Igneous Provinces: plate reconstructions, volcanic basins and sill volumes. *Geol. Soc. London, Spec. Publ.* **463**, 17–40. https://doi.org/10.1144/SP463.7.

Sweet, I.P., Mendum, J.R., Bultitude, R.J., Morgan, C.M. (1974a). The Geology of the Southern Victoria River Region, Northern Territory. *Bur. Miner. Resour. Geol. Geophys.* **Report 167**.

Sweet, I.P., Mendum, J.R., Morgan, C.M., Pontifex, I.R. (1974b). The Geology of the Northern Victoria River Region, Northern Territory. *Bur. Miner. Resour. Geol. Geophys.* **Report 166**.

Torsvik, T.H., Cocks, L.R.M. (2009). The Lower Palaeozoic palaeogeographical evolution of the northeastern and eastern peri-Gondwanan margin from Turkey to New Zealand. *Geol. Soc. London, Spec. Publ.* **325**, 3–21. https://doi.org/10.1144/SP325.2.

Torsvik, T.H., Cocks, L.R.M. (2017). Chapter 5: Cambrian, in: Torsvik, T.H., Cocks, L.R.M. (Eds.), *Earth History and Palaeogeography*. https://doi.org/10.1017/9781316225523.006.

Tucker, M.E. (1992). The Precambrian-Cambrian boundary: seawater chemistry, ocean circulation and nutrient supply in metazoan evolution, extinction and biomineralization. *J. Geol. Soc. London* **149**, 655–668.

Veevers, J.J. (2001). *Atlas of billion-year old earth history of Australia and neighbours in Gondwanaland*. GEMOC Press, Sydney, Australia.

Walter, M.R., Veevers, J.J. (1997). Australian Neoproterozoic palaeogeography, tectonics, and supercontinental connections. *J. Aust. Geol. Geophys.* **17**, 73–92.

Walter, M.R., Veevers, J.J., Calver, C.R., Grey, K. (1995). Neoproterozoic stratigraphy of the Centralian Superbasin, Australia. *Precambrian Res.* **73**, 173–195. https://doi.org/10.1016/0301-9268(94)00077-5.

Ware, B., Jourdan, F. (2018). $^{40}Ar/^{39}Ar$ geochronology of terrestrial pyroxene. *Geochim. Cosmochim. Acta* **230**, 112–136. https://doi.org/10.1016/j.gca.2018.04.002.

Ware, B.D. (2017). *Large Igneous Provinces of the Southern Hemisphere: Isotopic Geochemistry and Plagioclase and Pyroxene 40Ar/ 39Ar Geochronology of the Kalkarindji, Karoo and Ferrar Provinces*. PhD Thesis. Curtin University.

Ware, B.D., Jourdan, F., Merle, R., Chiaradia, M., Hodges, K. (2018). The Kalkarindji Large Igneous Province , Australia: Petrogenesis of the oldest and most compositionally homogenous province of the Phanerozoic. *J. Petrol.* **59**, 635–665. https://doi.org/10.1093/petrology/egy040

Webster, M., Gaines, R.R., Hughes, N.C. (2008). Microstratigraphy, trilobite biostratinomy, and depositional environment of the “lower Cambrian” Ruin Wash Lagerstätte, Pioche Formation, Nevada. *Palaeogeogr. Palaeoclimatol. Palaeoecol.* **264**, 100–122.

Wotte, T., Álvaro, J.J., Shields, G.A., Brown, B., Brasier, M.D., Veizer, J. (2007). C-, O-and Sr-isotope stratigraphy across the Lower–Middle Cambrian transition of the Cantabrian zone (Spain) and the Montagne Noire (France), West Gondwana. *Palaeogeogr. Palaeoclimatol. Palaeoecol.* **256**, 47–70.

Wotte, T., Skovsted, C.B., Whitehouse, M.J., Kouchinsky, A. (2019). Isotopic evidence for temperate oceans during the Cambrian Explosion. *Sci. Rep.* **9**, 6330.

Wotte, T., Strauss, H., Fugmann, A., Garbe-Schönberg, D. (2012). Paired δ34S data from carbonate-associated sulfate and chromium-reducible sulfur across the traditional Lower–Middle Cambrian boundary of W-Gondwana. *Geochim. Cosmochim. Acta* **85**, 228–253.

Zhang, W., Shi, X., Jiang, G., Tang, D., Wang, X. (2015). Mass-occurrence of oncoids at the Cambrian Series 2-Series 3 transition: Implications for microbial resurgence following an Early Cambrian extinction. *Gondwana Res.* **28**, 432–450. https://doi.org/10.1016/j.gr.2014.03.015.

Zhu, M., Zhuravlev, A.Y., Wood, R.A., Zhao, F., Sukhov, S.S. (2017). A deep root for the Cambrian explosion: Implications of new bio-and chemostratigraphy from the Siberian Platform. *Geology* **45**, 459–462.

Zhu, M.Y., Babcock, L.E., Peng, S.C. (2006). Advances in Cambrian stratigraphy and paleontology: Integrating correlation techniques, paleobiology, taphonomy and paleoenvironmental reconstruction. *Palaeoworld* **15**, 217–222. https://doi.org/10.1016/j.palwor.2006.10.016.

Zhu, M.Y., Zhang, J.M., Li, G.X., Yang, A.H. (2004). Evolution of C isotopes in the Cambrian of China: implications for Cambrian subdivision and trilobite mass extinctions. *Geobios* **37**, 287–301.

Zhuravlev, A.Y. (1996). Reef ecosytem recovery after the Early Cambrian extinction. *Geol. Soc. London, Spec. Publ.* **102**, 79–96. https://doi.org/10.1144/GSL.SP.1996.001.01.06.

Zhuravlev, A.Y., Wood, R.A. (1996). Anoxia as the cause of the mid-Early Cambrian (Botomian) extinction event. *Geology* **24**, 311–314. https://doi.org/10.1130/0091-7613(1996)024<0311.

Zhuravlev, A.Y., Wood, R.A. (2018). The two phases of the Cambrian Explosion. *Sci. Rep.* **8**, 1–10. https://doi.org/10.1038/s41598-018-34962-y.